Available online at www.sciencedirect.com
ScienceDirect
Polymer 48 (2007) 3844–3849
polymer
www.elsevier.com/locate/polymer

Nonisothermal crystallization behaviors of a polyolefin terpolymer and its foam

Yongsok Seo [a,*], Taejin Kang [a], Soon Man Hong [b], Hyoung Jin Choi [c]

[a] *Intellectual Textile Systems Research Center (ITRC), School of Materials Science and Engineering, College of Engineering, Seoul National University, Shillimdong 56-1, Kwanakku, Seoul 151-744, Republic of Korea*
[b] *Polymer Hybrid Research Center, Korea Institute of Science and Technology (KIST), P.O. Box 131, Cheongryang, Seoul 136-791, Republic of Korea*
[c] *Department of Polymer Science and Technology, Inha University, Yonghyun4dong, Namku, Inchon 402-751, Republic of Korea*

Received 5 December 2006; received in revised form 29 March 2007; accepted 15 April 2007
Available online 19 April 2007

Abstract

The nonisothermal crystallization kinetics of a polyolefin terpolymer (poly(propylene-*co*-ethylene-*co*-1-butene) and its expanded foam was investigated by differential scanning calorimetry. A kinetic equation for nonisothermal crystallization was employed to analyze the crystallization characteristics of the terpolymer and its foam. The Avrami exponent, n, can be reasonably well determined from the nonisothermal crystallization exotherm. The polarized optical microscopy showed that pristine terpolymer had a well-developed spherulite morphology whereas the foamed terpolymer consisted of elongated entities that subsequently developed as more bundle-like entities. The latter morphology is typical one of the γ phase. The difference in crystallization behavior observed for the pristine and foamed terpolymer samples is attributed to the formation of different morphologies during the foam expansion process.

Keywords: Nonisothermal crystallization; Terpolymer; Nucleation

1. Introduction

Polymer crystallization occurs via a nucleation and growth. In this process, the thermodynamic driving force provided by the supercooling of the amorphous melt causes the entangled polymer chains to rearrange into the ordered structures. Since the crystallization conditions decide the morphology, it is essential to understand the exact relationship between the structure and the stage of crystallization in processing. This is especially important for foamed structures, in which the crystallization simultaneously occurs. Despite a vast amount of research on crystallization, the nature of the crystallization process during foam formation remains unknown.

From the viewpoint of crystallization kinetics, the crystallization of isotactic polypropylene (iPP) is particularly interesting on account of this material's ability to form three distinct crystalline structures (i.e., polymorphism). Specifically, iPP crystallizes exclusively into a 3_1-helix structure as this conformation corresponds to an energy minimum, but with three forms, designated α, β, and γ [1–4]. The most common form of iPP is the α-form which has been well characterized by many researchers. The crystal cell of the α-iPP is monoclinic with parameters $a = 0.6657$ nm, $b = 2.096$ nm, $c = 0.65$ nm and $\beta = 99°80'$ consisting of alternating right- and left-handed helices [1]. The β-form iPP, by contrast, has a trigonal cell with parameters $a = b = 1.101$ nm and $c = 0.65$ nm containing three isochiral helices. Finally, the γ-form has a face-centered orthorhombic unit cell with parameters $a = 0.85$ nm, $b = 0.993$ nm and $c = 4.241$ nm containing no chiral helices [5–7]. The γ-form has a unique cell structure in which the chain axes in adjacent crystal layers are not parallel, rather the angle between the chains is about 80°. According to an extensive study by Alamo et al. [8], the stability of the γ-form, and hence its generation, depends on the total amount of stereo regulating

* Corresponding author. Tel.: +82 2 880 9085; fax: +82 2 885 9671.
E-mail address: ysseo@snu.ac.kr (Y. Seo).

0032-3861/$ - see front matter © 2007 Elsevier Ltd. All rights reserved.
doi:10.1016/j.polymer.2007.04.024

defects, mainly 2.1 and 3.1 insertions. The higher the defect concentration, the higher the maximum amount of the γ-form. Hence, addition of very short isotactic sequences induces a random distribution of stereo defects and/or regio defects in iPP samples synthesized using metallocene catalysts [2,6]. The terpolymer used in the present study consists mainly of an iPP structure with the addition of small amounts of ethylene and 1-butene units, which favors the formation of the γ-form. Since the γ phase is characterized by high molecular alignment and good mechanical properties, its presence is quite important to the final product performance [7]. The content of the γ-form in iPP can be increased in several ways [1] including (1) the presence of very short isotactic sequences due to the random distribution of stereo defects and/or regio defects in iPP samples synthesized by metallocene catalysts, (2) application of high pressure during the crystallization process, (3) using random copolymers of propene with other 1-olefins, and (4) crystallization in shear fields. Addition of other 1-olefins into the PP chain induces constitutional defects in the polymer chains. The content of the γ-form in an iPP sample depends on the amount and the type of comonomers. We have been interested in the generation of γ phase in iPP phase and its crystallization behavior.

Isothermal crystallization kinetics is normally analyzed using Avrami's equation. In an isothermal crystallization experiment, however, it is difficult to maintain the melt sample in an amorphous state while cooling it to the crystallization temperature. Moreover the crystallization processes encountered in nature tend to be nonisothermal. Nonisothermal crystallization kinetics has been theoretically explored by Ozawa [9,10], who extended the mathematical derivation first proposed by Evans [11]. However, Ozawa's theory has some limits [12,13]. Most of all, because this approach compares the degrees of conversion at a fixed temperature for various cooling rates, it can lead to deviations from the predicted linear behavior. We recently devised an analysis scheme in order to avoid the problem of the Ozawa analysis [14,15]. Since accounting for nonisothermal crystallization kinetics when analyzing crystallization can provide supplementary information about the crystal structure, it may give additional insight into the crystallite structures produced during foam formation. Hence, the objective of the present study was to apply our previously proposed nonisothermal analysis method to the crystallization behavior of a pristine terpolymer and its expanded (foamed) form with a focus on the morphological changes that occur during the foaming process.

2. Description of the theoretical model

Here, we briefly present the basic equations from our earlier report [14]. In the Ozawa equation, the Avrami equation is expressed using a cooling rate

$$\ln\left[-\ln\left(1-x_{\mathrm{v}}(T)_U\right)\right] = \ln K(T) - n\ln U \tag{1}$$

where $x_{\mathrm{v}}(T)$ is the volume fraction of the polymer transformed at a temperature T and cooling rate U, and $K(T)$ is the so-called cooling function, which only varies as a function of the temperature. Since the Ozawa equation is based on the volume fraction of the crystallites, conversion of the weight fraction of the polymer, $x_{\mathrm{w}}(T)$, to volume fraction of the polymer, $x_{\mathrm{v}}(T)$, is needed. This can be easily done by using the density of the amorphous phase and the density of the crystallized phase [9,15]. As suggested by the theory, a linear dependence between $\ln K(T)$ and the temperature T is assumed, $\ln K(T) = aT + b$. When the temperature reaches the peak of the exothermal curve, $T_{\max}$, for a given cooling rate, the first and the second derivatives of the curve with respect to the temperature should be zero. Using Eq. (1) with this condition, a linear relationship between $T_{\max}$ and $\ln U$ can be obtained, i.e., $n\ \ln U = aT_{\max} + b - \ln[-\ln(1 - x_{\mathrm{v}}(T_{\max})_U)]$. Therefore, Eq. (1) can be rewritten as

$$\ln\left[-\ln\left(1-x_{\mathrm{v}}(T)_U\right)\right] = a(T - T_{\max}) + \ln\left[-\ln\left(1 - x_{\mathrm{v}}(T_{\max})_U\right)\right] \tag{2}$$

Hence the value of the parameter a can be estimated from the slope of a plot of $\ln[-\ln(1 - x_{\mathrm{v}}(T)_U)]$ against $T - T_{\max}$. Also, plotting $T_{\max}$ versus $\ln U$ gives a straight line whose slope is n/a and intercept is $(\ln[-\ln(1 - x_{\mathrm{v}}(T_{\max})_U)] - b)/a$; thus, all the parameter values can be determined without resorting to any numerical process [15].

3. Experimental

The terpolymer (poly(propylene-*co*-ethylene-*co*-1-butene), with a composition of 94.5 wt% of polypropylene unit, 3 wt% of ethylene unit, and 2.5 wt% of 1-butene unit, was obtained from Honam Petrochemicals Co. (Korea). Its number and weight molar masses were 42,000 and 230,000 g/mol, respectively. Foamed terpolymer was prepared by injecting out the blowing agent (butane gas) submerged terpolymer particle in an autoclave through a nozzle. The expansion ratio (expanded pellet volume/pristine polymer volume) was 75. The thermal properties of the terpolymer samples were analyzed using differential scanning calorimetry (DSC), performed on a Mettler DSC 30. Prior to analysis, samples were dried at 100 °C in a vacuum oven for 24 h. About 45 mg of the dried terpolymer was used in each run. To examine nonisothermal crystallization, samples were heated from 25 °C to 200 °C at a heating rate of 100 °C/min, and then cooled at different cooling rates. Relative crystallinity was determined from the crystallization curve by DSC. The area under the curve from the crystallization starting temperature to each temperature was integrated. After divided by the total area, it was taken as the relative crystallinity.

A polarized optical microscope (Olympic BH-2) equipped with a Mettler FP82 HT hot stage and a CCD camera was used to record the growth of the crystallites. Crystal structure analysis was performed using an X-ray diffractometer (XRD) of Rigaku Denki D/Max 2000. X-ray diffraction patterns were recorded using Cu Kα radiation from a rotating anode X-ray goniometer operating at 40 kV and 100 mA equipped with an automatic monochromator.

4. Results and discussion

In Ozawa's approach, the rates of conversion to crystalline phase at various temperatures are compared. However, since the crystallization processes proceeding under different cooling rates will be at different stages, this approach can lead to substantial curvature in the Ozawa plots [14]. As a result, Ozawa's approach is inappropriate for modeling nonisothermal crystallization [13]. By contrast, our approach can select the relative crystallinity at the same cooling rate and does not include values from the other rates [14]. The validity of our approach has been established in our previous reports [14,16]. In the present work, we sought to elucidate the morphological changes that occurred during the foaming process.

Fig. 1 displays a linear variation of the maximum temperature of the terpolymer crystallization isotherm, T_{max}, with the logarithm of the cooling rates ($\ln U$). The predicted behavior is observed provided the cooling rate is low (<7 °C/min). T_{max} decreases with increasing cooling rate because less time is available for crystallization at higher cooling rates. These findings show that our modified version of the Ozawa's theory is quite satisfactory.

Fig. 2 displays the relative crystallinity of pristine terpolymer as a function of temperature for various cooling rates. At higher cooling rates, a large fraction of the relative crystallinity occurs after the most rapidly increasing point in the heat flow curve, where the kinetics begins to change to a slower process. The plot of $\ln[-\ln(1-x_v(T)_U)]$ versus $(T-T_{max})$, as shown in Fig. 3, gives a straight line with a slope of n/a. The calculated values of the Avrami exponent, n, are between 2.6 and 3.7, with an average value of 3.1 (Table 1). This value is close to the characteristic value for spherulitic development arising from athermal instantaneous nucleation [14]. These findings thus suggest that spherulites develop during nonisothermal crystallization of the terpolymer, which, as will be seen below, is consistent with the morphologic data obtained for these systems. Fig. 4 shows the variation of T_{max} as a function of $\ln U$ for the foamed terpolymer. This system also shows a good linear relationship between T_{max} and $\ln U$ at low cooling rates.

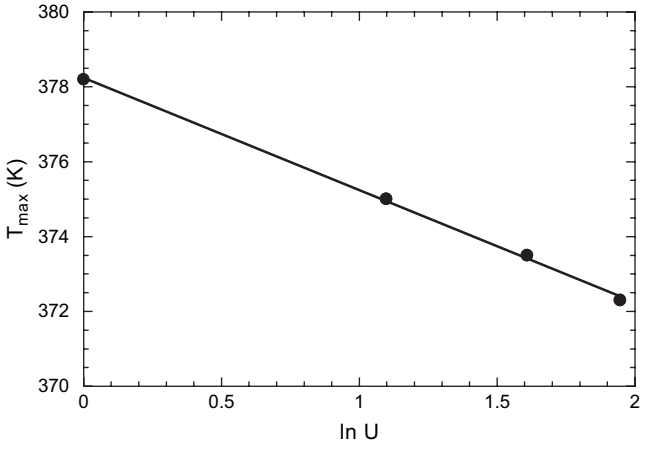

Fig. 1. Evolution of T_{max} of virgin terpolymer as a function of $\ln U$ (U is the cooling rate). The slope of the solid line is −3.0 which is the value of n/a.

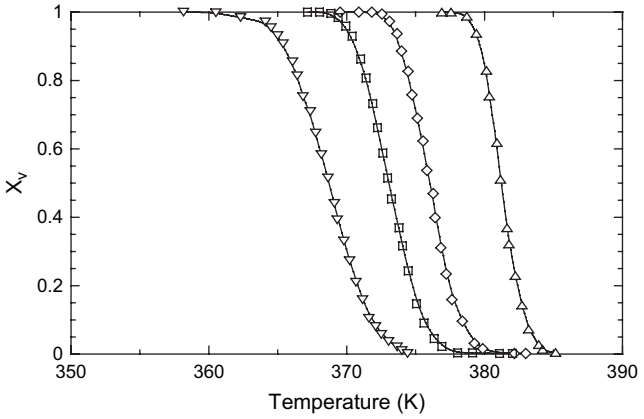

Fig. 2. Development of relative crystallinity with temperature for nonisothermal crystallization of virgin terpolymer at various cooling rates. (△) 1 K/min, (◇) 3 K/min, (□) 5 K/min, (▽) 7 K/min.

Again, because less time is available for crystallization at higher cooling rates, T_{max} decreases as the cooling rate increases. T_{max} of the foamed terpolymer is higher than that of the pristine terpolymer at the same cooling rate, indicating a faster crystallization for the foamed terpolymer. Fig. 5 shows the relative crystallinity of the foamed terpolymer plotted as a function of temperature for various cooling rates. Consistent with the behavior of T_{max}, the relative crystallinity data indicate that the foamed terpolymer crystallizes faster than the pristine terpolymer, especially at higher cooling rates. The observation of faster crystallization for the foamed terpolymer can be attributed to the existence of a greater density of nuclei in the

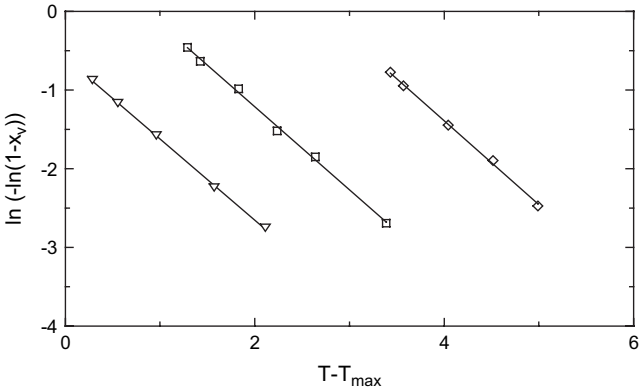

Fig. 3. Plot of $\ln[-\ln(1-x_v(T)_U)]$ versus $T-T_{max}$ for nonisothermal crystallization of virgin terpolymer. (▽) 1 K/min, (□) 3 K/min, (◇) 5 K/min.

Table 1
Peak temperature T_{max} of virgin terpolymer and foamed terpolymer and their Avrami exponent values (n)

Cooling rate (K/min)	Virgin terpolymer		Foamed terpolymer	
	T_{max} (K)	n	T_{max} (K)	n
1	378.2	3.3	382.6	6.47
3	375.0	3.1	376.2	6.1
5	373.5	3.05	373.2	5.35
Average		3.15 ± 0.13		5.65 ± 0.26

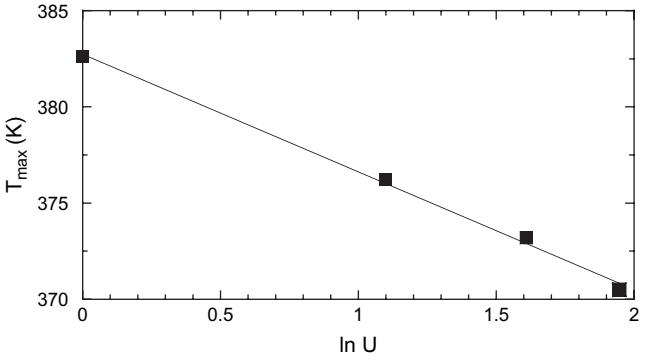

Fig. 4. Evolution of T_{max} of foamed terpolymer as a function of ln U (U is the cooling rate). The slope of the solid line is −6.1 which is the value of n/a.

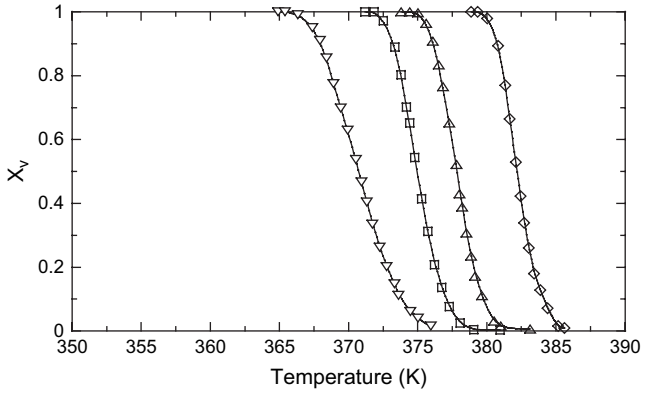

Fig. 5. Development of relative crystallinity with temperature for nonisothermal crystallization of PEEK at various cooling rates. (◇) 1 K/min, (△) 3 K/min, (□) 5 K/min, (▽) 7 K/min.

foamed terpolymer than in the pristine terpolymer. The foaming process is a mixed process of elongational flow with shear deformation. In a recent study of crystallization in a flow field, Grizzuti et al. [17] proposed a model that includes the effect of a flow field on the crystallization. Subsequently, they showed that this model can predict the effect of a flow field on crystallization. In particular, they showed that the presence of even a small amount of elongational flow component can have an enormous effect on the nucleation rate [18]. The difference between the effects of elongational flow and shear flow on the nucleation rate is more remarkable for highly elastic fluids. Specifically, forcing the molecular chains to flow past one another causes them to be in a more ordered state thereby creating more nuclei for crystallization. This process is referred to as flow induced crystallization (FIC). The ordering of macromolecules occurs more easily under elongational deformation than under shear flow because elongational flow is a strong deformation [18]. Since the foaming process is a mixture of elongational and shear deformations [19], a large number of nuclei may be generated during foaming. Blowing agent induced crystallization can be ruled out because of gas-induced plasticization effect for iPP [20]. Zhang et al. recently reported that decreasing the melt-crystallization temperature can delay polymer crystallization, favoring cell growth for conventional frames in the polymer foam extrusion [20]. In our previous study on the isothermal crystallization kinetics of the same terpolymer as used here, we calculated the nucleation density number [21]. Our results showed that for crystallization temperatures of 100–107 °C, the foamed resin contained about three times more nuclei than the pristine terpolymer and that the difference in nucleation density between the foamed and the pristine samples increased rapidly with decreasing crystallization temperature. Thus, it is reasonable to infer that crystallization of the foamed terpolymer proceeds mainly via self-nucleation whereas that of the pristine terpolymer proceeds both by self-nucleation and homogeneous nucleation mechanisms [22,23]. Moreover, we found that even if the samples were heated to 200 °C, some ordered structures still remained that could act as the self-nucleation sites when the sample was subsequently cooled.

The faster crystallization of the foamed terpolymer due to its large number of nuclei leads to a greater number of defects in the crystallized terpolymer. These defects would contribute to the formation of the γ-form. The data published so far indicate that when the fully isotactic sequences are very short, iPP crystallizes in the γ-form whereas the very long regular isotactic sequences generally crystallizes exclusively in the α-form [1–3,6]. Mandelkern et al. reported that the distribution of defects in iPP produced by a Ziegler–Natta (ZN) catalyst was not random, but rather defects were more concentrated in the molecules with the low molar mass [6]. As a result of this bias in the defect distribution, iPP produced using a ZN-catalyst crystallized into the γ phase to a much lesser extent than did in iPP sample synthesized using a metallocene catalyst with the same overall concentration of defects. The large number of nuclei in the foamed terpolymer and their more uniform distribution throughout the sample makes the concentration of crystallizable sequences of polymer molecules exceed the required length for a nucleus of critical size, which results in the formation of more defects during the ordering process. Therefore, the γ phase could be expected to be formed more easily in the foamed terpolymer than in the pristine terpolymer. The calculated average value of Avrami exponent, n, from Fig. 6 is *ca* 5.6 for the foamed terpolymer (Table 1). This large exponent implies a solid sheaf morphology [23]. The morphologies of the foamed one and pristine one are shown in Fig. 7. They are completely different

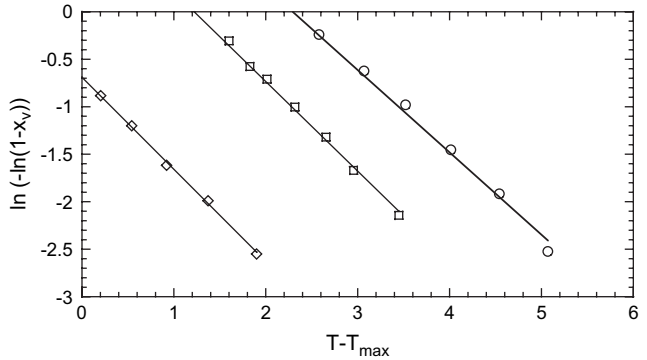

Fig. 6. Plot of ln[−ln(1 − $x_v(T)_U$)] versus $T - T_{max}$ for nonisothermal crystallization of foamed terpolymer. (◇) 1 K/min, (□) 3 K/min, (○) 5 K/min.

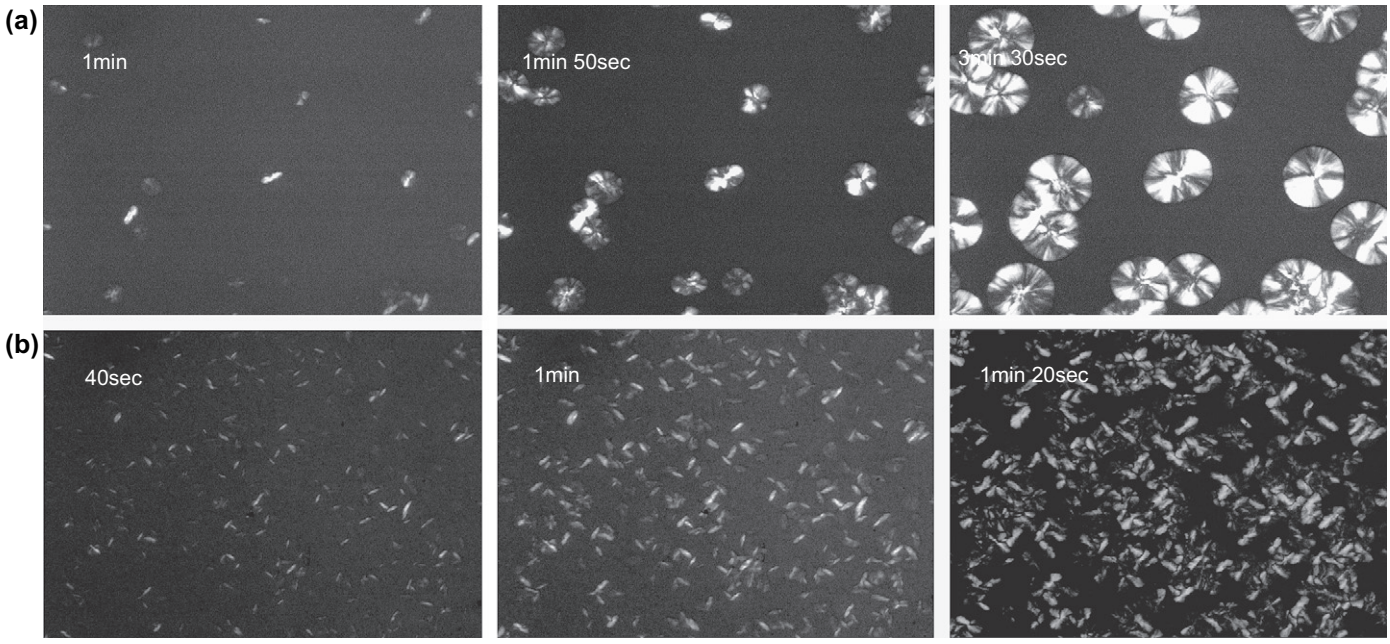

Fig. 7. Polarized optical micrographs taken after nonisothermal crystallization of (a) a virgin terpolymer (poly(propylene-*co*-ethylene-*co*-1-butene) and (b) foamed terpolymer at a cooling rate of 1 K/min.

from each other. The pristine terpolymer (Fig. 7(a)) shows a well-developed spherulite, later limited by several adjacent ones, typical crystalline structure of the iPP. On the other hand, the foamed terpolymer (Fig. 7(b)) shows elongated entities, that later develop as more bundle-like entities. This is a typical morphology of the γ phase [1,2]. Some small spherulites were subsequently formed between the extended entities during the cooling process. The morphological difference is consistent with the number density difference of nuclei. This is rather similar to the nonisothermal crystallization behavior of poly(ether ether ketone) (PEEK) [14]. In our previous study on the nonisothermal crystallization kinetics of PEEK, we observed sheaf-like growth of the PEEK crystallites and a high Avrami index. However, PEEK develops a hedrite structure rather than the cylindrulite structure, although these two structures are indistinguishable in the early stages of crystallization. A similar morphology was observed for isotactic polypropylene synthesized using a metallocene catalyst and isothermally crystallized at 120 °C for a long time (more than 48 h) [2]. Most of the polymer was in the γ-form. For isotactic polypropylene, it was obvious that a change from chain-folded crystallization to extended chain crystallization occurred.

Formation of the γ-form could be confirmed by checking WAXD analysis of the samples. Fig. 8 shows the WAXD traces of the as-prepared pristine terpolymer and the foamed one. The α- and γ-forms give rise to very similar X-ray diffraction profiles, with the main difference being the position of the third strong diffraction peak, which occurs at $2\theta = 18.6$ ($(130)_\alpha$ reflection) for the α-form and at $2\theta = 20.1$ ($(117)_\gamma$ reflection) for the γ-form [2]. The 117 peak of the γ phase appears weakly in the pristine terpolymer sample but strongly for the foamed terpolymer. For the foamed terpolymer sample, the 130 peak of the α phase appears weakly compared to that of the 117 peak. The ratio of the γ phase to the α phase is usually determined by the method of Turner-Jones [24]. In this method, the ratio is directly calculated from the ratio of the height of the (130) reflection of the α phase (h_α) to that of the (117) reflection of the γ phase (h_γ). The γ phase contents are then given by $x_\gamma = h_\gamma/(h_\alpha + h_\gamma)$. Using this calculation, we found that the as-prepared foamed sample showed a high content of the γ-form, almost 65%. The γ phase content decreased with decreasing cooling rates.

The cooling function, K, changes as a function of temperature, which is attributable to changes in the growth rate and the nucleation density. For mathematical convenience, we assumed that K followed the relationship, $\ln K(T) = aT + b$. If we adopt an Arrhenius form for $K(T)$, the activation energy for crystallization of the terpolymer and its foam under

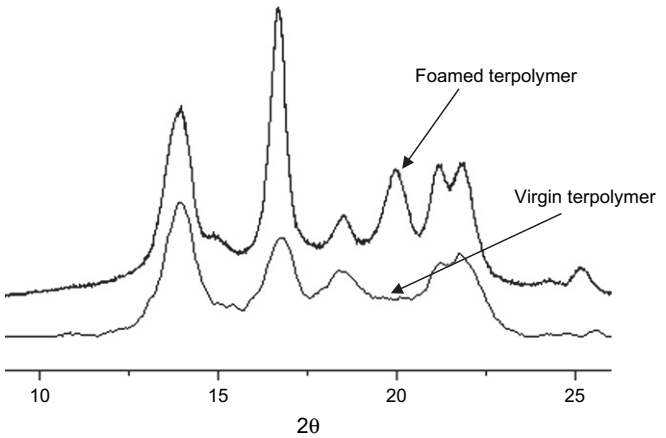

Fig. 8. WAXD traces of samples as prepared. Expansion ratio of the foamed sample was 75 times.

nonisothermal conditions at low degrees of conversion (<0.4 in this study) can be determined [14]. Because of dimensional differences due to variations in the values of n, the rate parameters obtained at different cooling rates cannot be directly compared [13]. Rather, the K values for various cooling rates should be normalized to allow a fair comparison on a common basis as $K^{1/n}$. Then, it can be written in the Arrhenius form as the nonisothermal crystallization rate constant, $K^{1/n} = K_0 \exp(-\Delta E/RT)$, where K_0 is a temperature-independent pre-exponential and ΔE is the activation energy. Taking the logarithm of both sides and comparing values of K at two different temperatures but at the same cooling rate, we obtain

$$\frac{1}{n}\ln\frac{K_2}{K_1} = -\frac{\Delta E}{R}\left(\frac{1}{T_2}-\frac{1}{T_1}\right) = \frac{\Delta E}{R}\left(\frac{T_2-T_1}{T_1T_2}\right) \quad (3)$$

Thus, the activation energy can be calculated using values of K obtained at different temperatures of the same isotherm. As long as the conversion is in the very low range, the Arrhenius form is suitable for nonisothermal experimental results [13]. Since the temperature difference at a low degree of conversion (<0.4) is less than 5 °C when the cooling rate is less than 7 °C/min (Fig. 2), the activation energy was obtained with an error range of ±5% and its average value was *ca* −40.3 kcal/mol for the pristine terpolymer. This is little bit smaller but close to that of pure iPP (−44.7kcal/mol) [25]. On the other hand, the activation energy of the foamed terpolymer was −27.3 kcal/mol, which is much smaller than the values for iPP and the pristine terpolymer, consistent with the very fast crystallization of the foamed terpolymer due to a large density of nuclei in the sample.

5. Conclusions

Nonisothermal crystallization analysis of a terpolymer and its foam provides some important information about the crystalline structures of these materials. In the present work, a modified version of the Ozawa's method proposed by us was successfully applied to the DSC data of a polypropylene containing terpolymer and its foam at various low cooling rates. The Avrami exponent of the pristine terpolymer was 3.1, which is close to that of iPP, indicating that the crystallites had a spherulite structure. On the other hand, high Avrami exponent values (*ca* 5.6) were obtained for the foamed terpolymer, indicating that the crystallites had structures resembling a three dimensional solid sheaf. This difference between the pristine and foamed terpolymer samples is attributed to the appearance of the γ-form in the foamed terpolymer. Observation of the morphologies of these materials as well as crystallographic analysis confirmed these findings. The morphology of the pristine terpolymer was spherulites whereas that of the foamed terpolymer consisted of bundle-like structures. In addition, a strong peak characteristic of the γ-form ($(117)_\gamma$) was observed in the WAXD pattern of the foamed terpolymer. The observed behavior can be attributed to a large number of nuclei being produced during the foaming process by FIC. For the foamed terpolymer of large number of nuclei, the chain length is too long for a stable crystallite formation. This leads to more defects in the molecule and hence, to more γ-form formation. The activation energy of the crystallization process was −40.3 kcal/mol for the pristine terpolymer and −27 kcal/mol for the foamed terpolymer. The lower activation energy of the foamed terpolymer implies that it undergoes faster crystallization due to the large density of nuclei in the sample.

Acknowledgements

This work was partly supported by KRF (0417-20060134, Seo), the SRC/ERC program of MOST/KOSEF (R11-2005-065, Kang), KOSEF (R01-2006-000-10062-0, Choi), and 21C Frontier Research Fund for Resources Recycling Program (0417-20050058, Hong).

References

[1] Kressler J. In: Karger-Kocsis J, editor. Polypropylene. Kluwer Academic; 1991. p. 267.
[2] Thomann R, Wang C, Kressler J, Műllhaupt R, Robeson R. Macromolecules 1996;29:8425.
[3] Aurienma F, De Rosa C, Boscato T, Corradive P. Macromolecules 2001; 34:4815.
[4] Huo H, Jiang S, An L, Feng J. Macromolecules 2004;37:2478.
[5] Bruckner S, Meille SV. Nature (London) 1989;340:455.
[6] Hosier IL, Alamo RG, Exteso P, Isasi JR, Mandelkern L. Macromolecules 2003;36:5623.
[7] Phillips RA, Wolkowicz MD. In: Moor EP, editor. Polypropylene handbook. Munich: Hanser; 1996 [chapter 3].
[8] Alamo K, Vander Hart DL, Nyden MR, Madelkern L. Macromolecules 2000;35:6094.
[9] Ozawa T. Polymer 1971;12:150.
[10] Nakamura N, Watanabe T, Kotayama K, Amano T. J Appl Polym Sci 1972;16:1077.
[11] Evans UR. Trans Faraday Soc 1941;41:365.
[12] Srinivas S, Babu JR, Riffle JS, Wilkes GL. Polym Eng Sci 1997;37:497.
[13] Cebe P, Hong S. Polymer 1986;27:1183.
[14] Seo Y, Kim S. Polym Eng Sci 2001;41:940.
[15] Verohyen O, Dupret F, Legas R. Polym Eng Sci 1998;38:1594.
[16] Seo Y. Polym Eng Sci 2000;40:1293.
[17] Acierno S, Grizzuti N, Winter HH. Macromolecules 2002;35:5043.
[18] Acierno S, Coppola S, Grizzuti N, Maffetone P. Macromol Symp 2002; 185:233;
Coppola S, Grizzuti N. Macromol Symp 2004;218:137.
[19] Edwards DA, Wasan DT. In: Prud'homme RK, Khan SA, editors. Foams Surfactant science series, vol. 57. Marcel Dekker; 1996. p. 189–216.
[20] Zhang Z, Nawaby AV, Day M. J Polym Sci Part B Polym Phys 2003; 41:1518.
[21] Seo Y, Kang T, Hwang J, Hong S. J Phys Chem B 2007;111:3571.
[22] Seo Y, Kim J, Kim KU, Kim YC. Polymer 2000;41:2639.
[23] Wunderlich B. In: Turi A, editor. Thermal characterization of polymeric materials. Academic Press; 1997 [chapter 2].
[24] Turner-Jones A. Polymer 1971;12:487.
[25] Wang L, Sheng J. J Macromol Sci Part B Phys 2005;44:31.